Electronic Supplementary Material (ESI) for Journal of Materials Chemistry C.

Supporting information for

Multiple spin phases in a switchable Fe(II) complex: polymorphism and symmetry breaking effects

Hao Hang,[a] Bin Fei,[a] Xiu Qin Chen,[a] Ming Liang Tong,[b] Vadim Ksenofontov,[c] Il'ya A. Gural'skiy*[d] and Xin Bao*[a]

[a] School of Chemical Engineering, Nanjing University of Science and Technology, 210094 Nanjing, P. R. China

[b] Key Laboratory of Bioinorganic and Synthetic Chemistry of Ministry of Education, School of Chemistry, Sun Yat-Sen University, 510275 Guangzhou, P. R. China.

[c] Dr. Vadim Ksenofontov, Institute of Inorganic and Analytical Chemistry, Johannes Gutenberg University of Mainz, Duesbergweg 10-14, 55099 Mainz, Germany

[d] Dr. Il'ya A. Gural'skiy, Department of Chemistry, Taras Shevchenko National University of Kyiv, 64 Volodymyrska St., Kyiv 01601, Ukraine

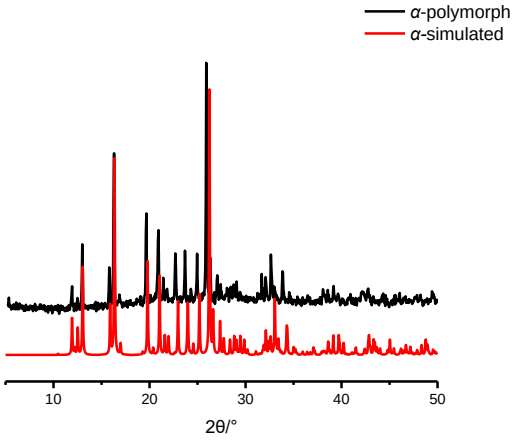

Figure S1. Experimental and simulated PXRD patterns of the ***α***-polymorph.

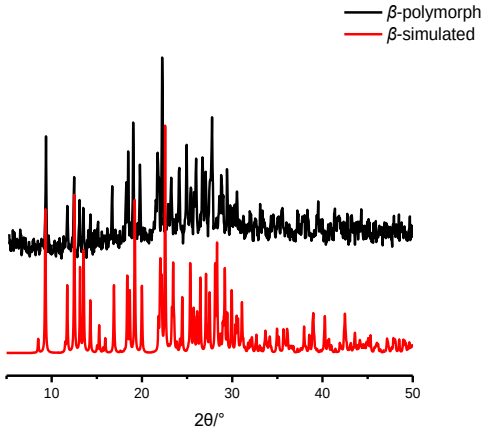

Figure S2. Experimental and simulated PXRD patterns of the ***β***-polymorph.

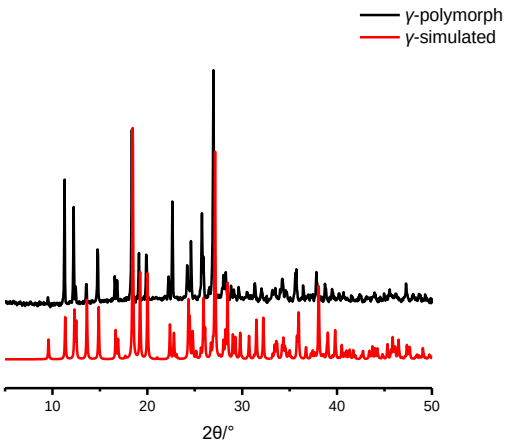

Figure S3. Experimental and simulated PXRD patterns of the ***γ***-polymorph.

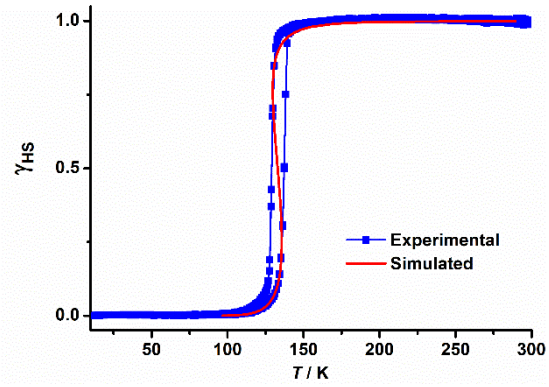

Figure S4. Simulated SCO curve for the spin transition in alpha-polymorph. Regular solution model (Kahn, O. Molecular Magnetism. *J. Chem. Educ.* **1995**, *72* (1), A19)) was used to reproduce the HS spices content vs. temperature. Parameters of the simulation: ΔH=15.7 kJ/mol, Γ =3000 kJ/mol, T = 133 K. The deviation of ΔH from the DSC experiment are originated from the simplicity of the model (e.g., domains are not considered). Γ value is higher than 2RT=2212 kJ/mol, which leads to the hysteretic spin transition.

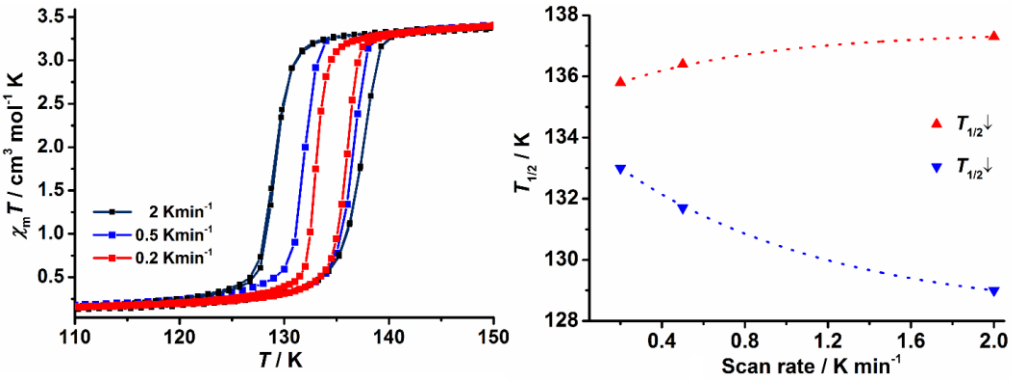

Figure S5. Left: Temperature dependence of the $\chi_M T$ product for the ***α***-form at three different scan rates between 110 and 150 K. Right: The observed $T_{1/2}\downarrow$ (cooling) and $T_{1/2}\uparrow$ (heating) values as a function of the scan rate. The dotted lines are for guiding the eyes.

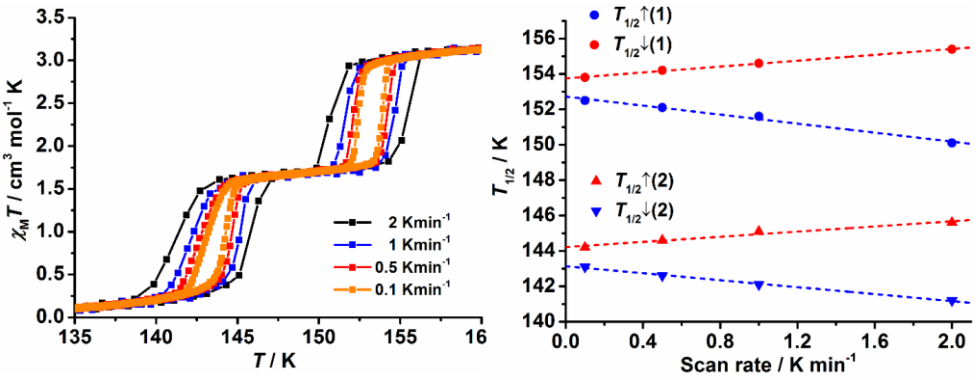

Figure S6. Left: Temperature dependence of the $\chi_M T$ product for the ***β***-form at four different scan rates between 130 and 160 K. Right: The observed $T_{1/2}\downarrow$ (cooling) and $T_{1/2}\uparrow$ (heating) values as a function of the scan rate. The dotted lines correspond to the linear fit.

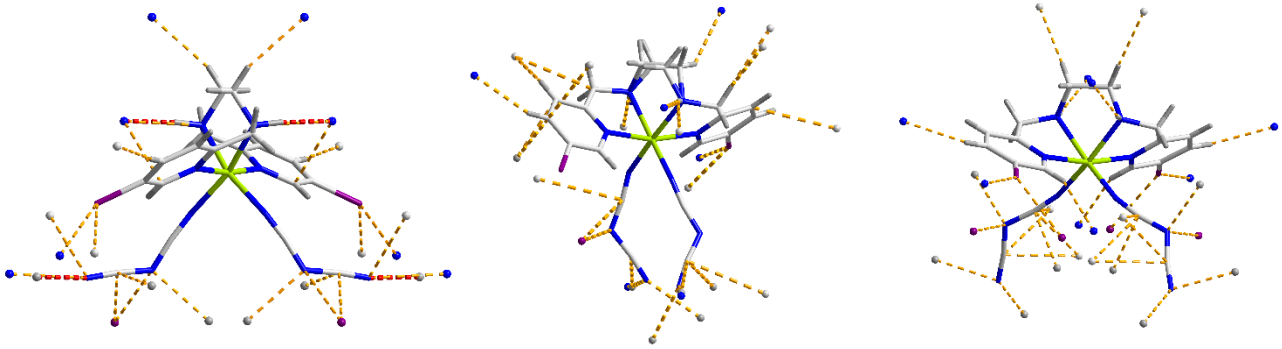

Figure S7. Intermolecular interactions exhibited by α (left), β (middle) and γ (right) forms of the $[FeL_{Br}(dca)_2]$ complex in their HS phase.

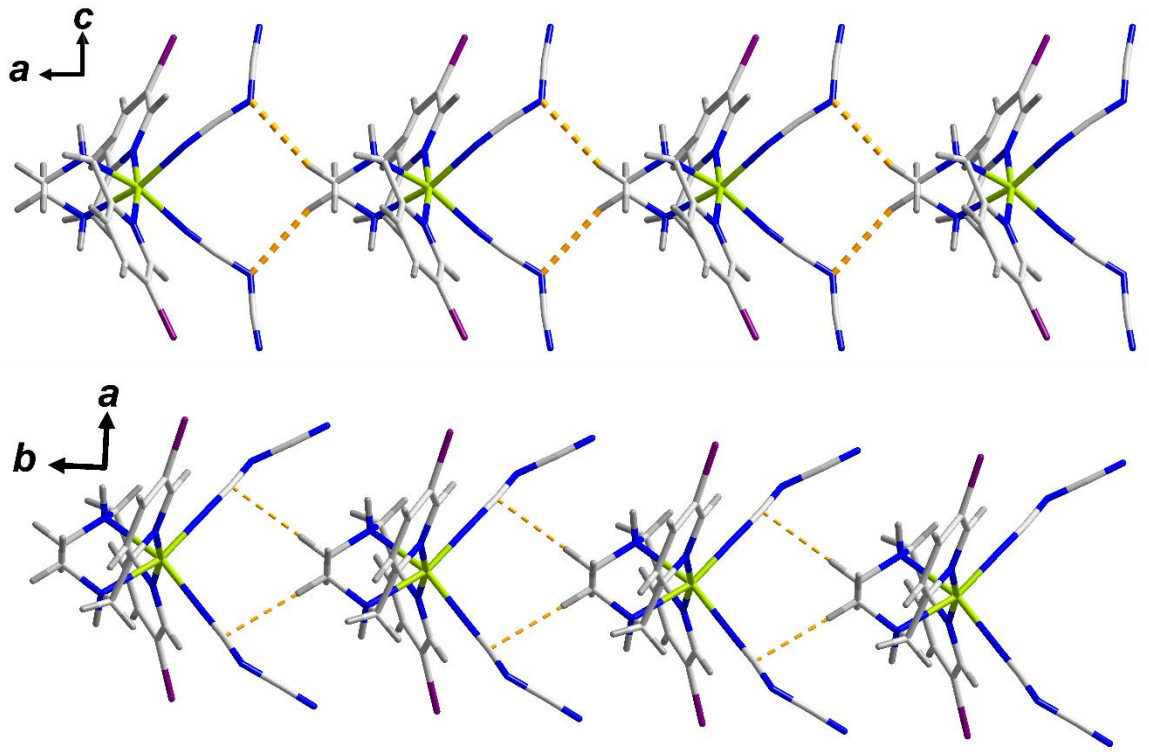

Figure S8. Two dca arms in a $[FeL_{Br}(dca)_2]$ complex embraces a $NHCH_2CH_2NH$ backbone of the neighbouring complex, forming a 1D linear supramolecular organization in α-form (top) and γ-form (down). Color code: C, light grey; H, grey; Fe, green; N, blue; Br, violet. Van der Waals interactions are indicated by dotted lines.

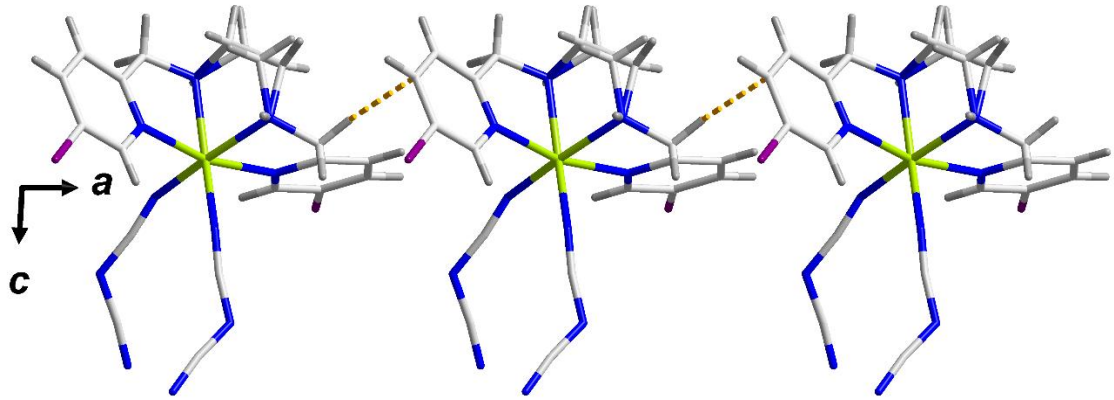

Figure S9. C-H(methylene)···C(pyridine) short interactions (orange dotted lines) give rise to a 1D chain along the *a* axis in ***β***-form. Color code: C, light grey; H, grey; Fe, green; N, blue; Br, violet.

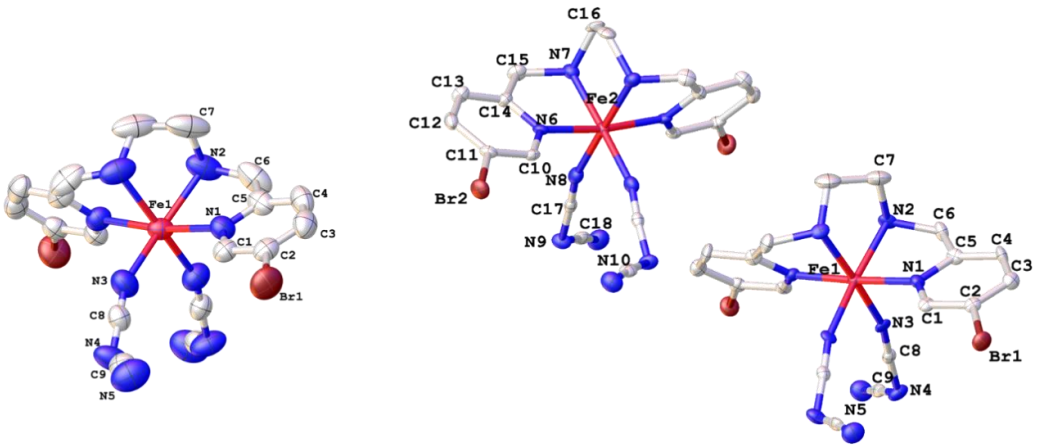

Figure S10. View of the molecular structures in ***α***-form at 298 K (left) and 123 K (right). Hydrogen atoms are deleted for clarity. Thermal ellipsoids are presented at 50% probability. Color code: Fe, red; C, grey; Br, brown; N, blue.

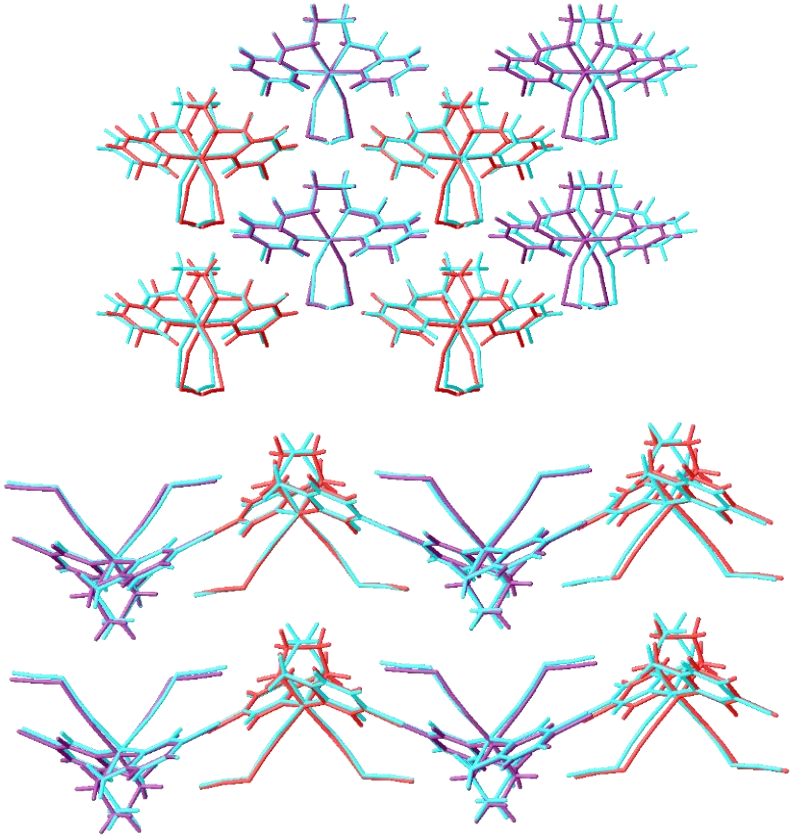

Figure S11. Overlay of the packing structures in ***α***-form at 298 K (in blue) and 123 K (Fe1 in purple and Fe2 in red) in *ab* (top) and *ac* (bottom) planes.

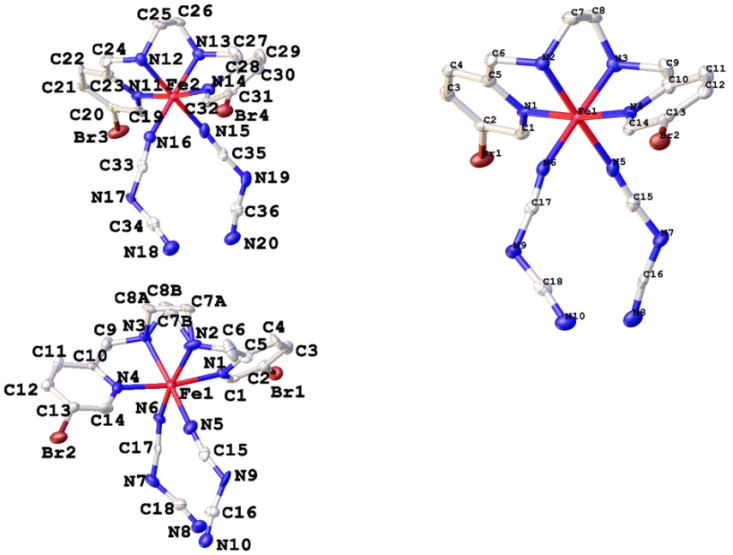

Figure S12. View of the molecular structures in ***β***-form at 146 K (left) and 123 K (right). Hydrogen atoms are deleted for clarity. Thermal ellipsoids are presented at 50% probability. Color code: Fe, red; C, grey; Br, brown; N, blue.

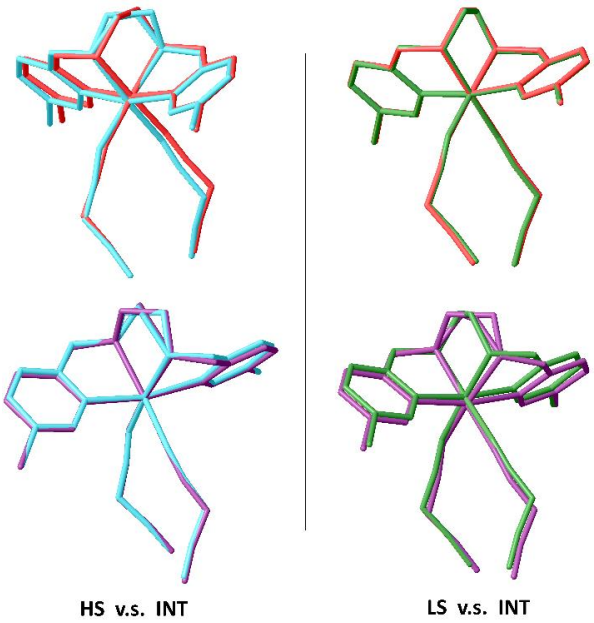

Figure S13. Overlay of the molecular structures of the Fe(II) complexes in ***β***-form at different temperatures. Left: 298 K (blue) vs. 146 K (Fe1 site in red and Fe2 site in purple); Right: 123 K (green) vs. 146 K (Fe1 site in red and Fe2 site in purple). Fe1 sites are forced to be overlaid and two neighbouring Fe1 sites at 298/123 K were shown in order to compare with the two distinct Fe sites at 146 K.

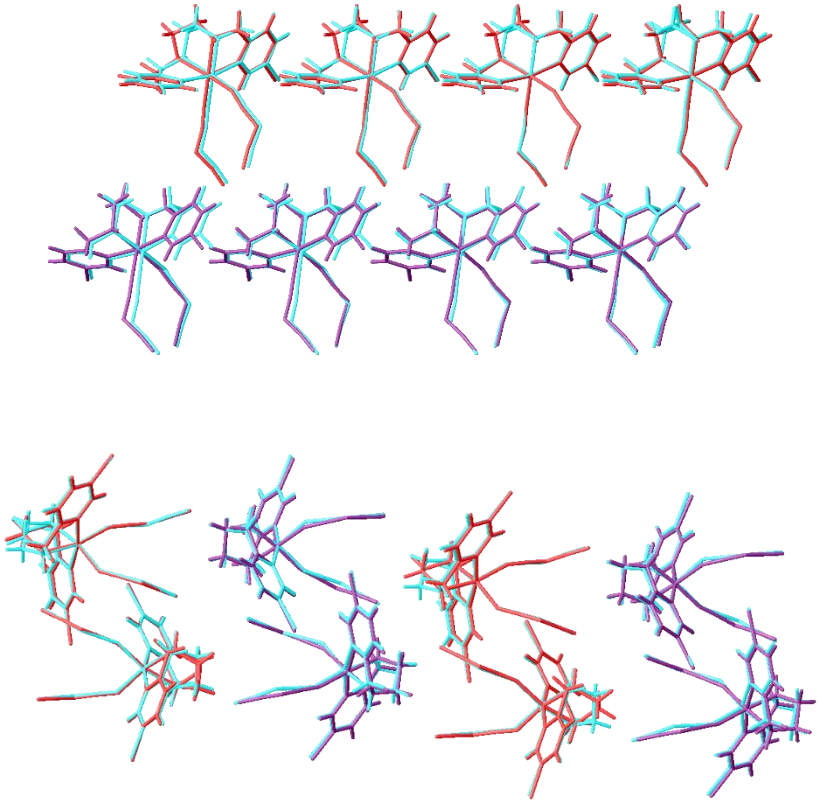

Figure S14. Overlay of the packing structures in ***β***-form at 298 K (in blue) and 146 K (Fe1 in purple and Fe2 in red) in *ac* (top) and *bc* (bottom) planes.

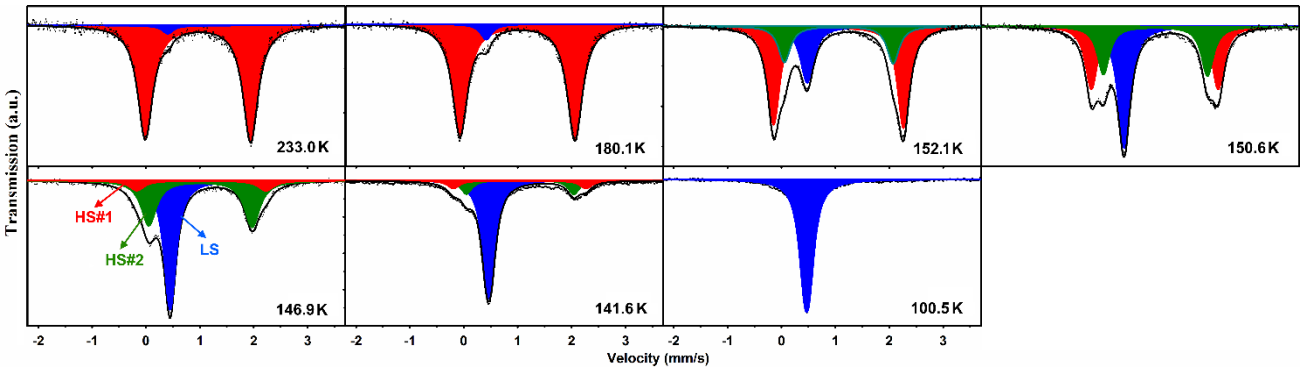

Figure S15. ^{57}Fe Mössbauer spectra of the ***β***-form recorded in the 233-100 K temperature range. The spectra are deconvoluted into subspectra corresponding to HS #1 (red), HS #2 (green) and LS (blue) sites.

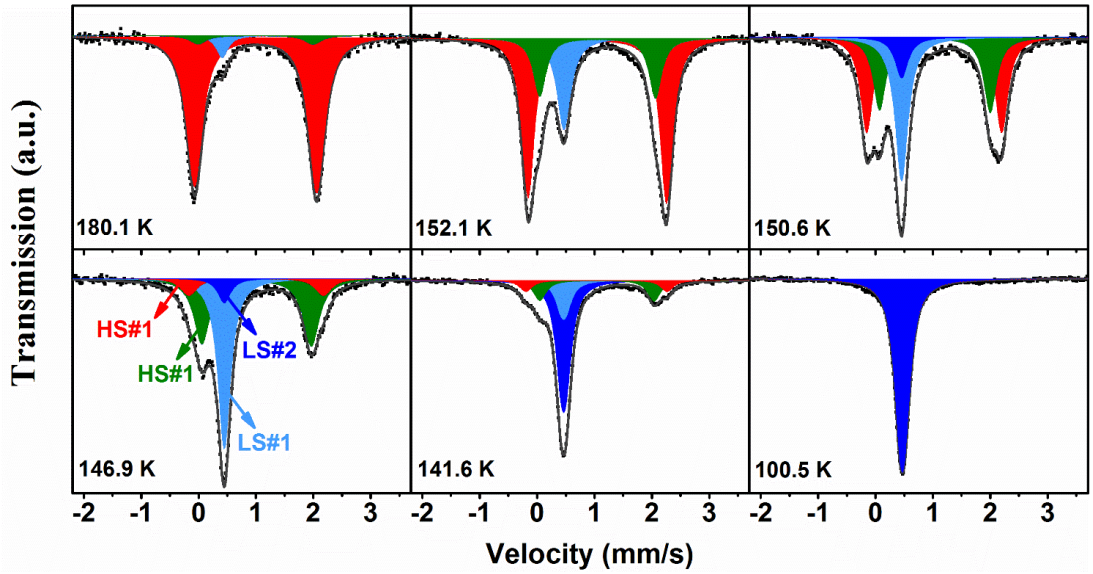

Figure S16. Alternative fitting for ^{57}Fe Mössbauer spectra of the ***β***-form. The spectra are deconvoluted into subspectra corresponding to HS #1 (red), HS #2 (green), LS #1 (cyan) and LS #1 (blue) sites.

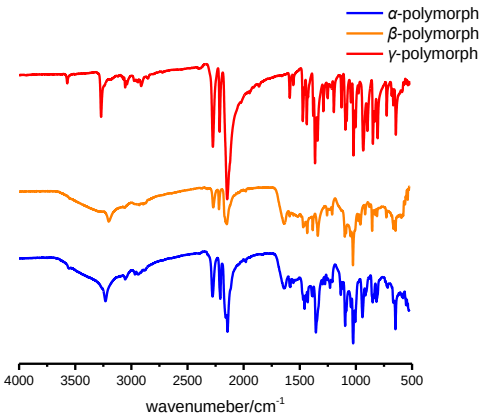

Figure S17. IR spectra for ***α–γ*** polymorphs in the region of 4000–525 cm^{-1} at room temperature.

Table S1. Selected supramolecular interactions in the ***α***-form.

	298 K		123 K	
			N5-N7	2.971(11) Å
H bond	N5-N2	2.941(9) Å	N5-H7-N7	178.3(4) º
(CN···H-N)	N5-H2-N2	168.0(4) º	N10-N2	2.911(12) Å
			N10-H2-N2	155.5(5) º
H bond	N4-C7	3.557(10) Å	N4-C7	3.560(13) Å
(dca···ethylene)	N4-H7A-C7	159.8(5) º	N4-H7B-C7	177.6(6) º
			N9-C16	3.507(11) Å
			N9-H16A-C16	146.1 (5)

Table S2. Selected supramolecular interactions in the ***β***-form.

	298 K		146 K		123 K	
	N10-N3	3.055(13) Å	N10-N3	3.082(15) Å	N10-N3	2.995(6) Å
	N10-H3-N3	170.9(6) º	N10-H3A-N10	169.0(6) º	N10-H3-N3	172.7(3) º
			N20-N12	2.988(15) Å		
H bond			N20-H12A-N12	174.0(6) º		
(CN···H-N)	N8-N2	3.018(12) Å	N18-N13	3.032(15) Å	N8-N2	2.995 (6) Å
	N8-H2-N2	155.6(5) º	N18-H13-N13	172.9(7) º	N8-H2-N2	172.9(2) º
			N8-N2	3.118(16) Å		
			N8-H2-N2	170.9(7) º		
	Br1-N9	3.202(10) Å	Br4-N17	3.291(11) Å	Br2-N9	3.242(5) Å
Halogen bond	C13-Br1-N9	157.6(3) º	C31-Br4-N17	158.7(4) º	C13-Br2-N9	159.52(18)º
(Br···dca)			Br1-N7	3.163(12) Å		
			C2-Br1-N7	160.4(4) º		
	C3-H9B	2.605(10) Å	C12-H6B	2.543(12) Å	C3-H9A	2.566(5) Å

Table S3. Selected supramolecular interactions in the ***γ***-form.

	298 K		123 K	
H bond (CN···H-N)	N5-N2	3.245(7) Å	N5-H2	3.169(5) Å
	N5-H2-N2	144.0(3) º	N5-H2-N2	143.7(2)
dca···ethylene	C8-H7A	2.651(6) Å	C8-H7B	2.586(4) Å
Br···Br	Br-Br	3.678(11) Å	Br-Br	3.6229 (7)

Table S4. Alternative fitting parameters for Mössbauer spectra of the ***β***-form.

T / K		233	180.1	152.1	150.6	146.9	141.6	100.5
HS#1	δ / mm s^{-1}	0.9677	0.9940	1.051(13)	1.0227	1.004	1.0438	--
	ΔE_Q / mm s^{-1}	1.961(7)	2.1308	2.409(4)	2.3523	2.345	1.992	--
	Linewidth / mm s^{-1}	0.1718	0.1737	0.1359[a]	0.1359	0.1718	0.1359	--
	Fraction / %	93.8	90.0	59.7(9)	36.1	10.9	9.4	--
HS#2	δ / mm s^{-1}	0.9677	0.9940	1.054(4)	1.0356	1.011	1.0365	--
	ΔE_Q / mm s^{-1}	1.7 (2)	2.00(8)	2.02(11)	1.9303	1.909	2.458	--
	Linewidth / mm s^{-1}	0.1718	0.1737	0.1359[a]	0.1359	0.1718	0.1359	--
	Fraction / %	3.6	5.2	21.9(9)	28.1	41.3	17.1	--
LS#1	δ / mm s^{-1}	0.4105	0.411	0.47(3)	0.4551	0.4479	0.4620	--
	ΔE_Q / mm s^{-1}			--			0.0913	--
	Linewidth / mm s^{-1}	0.127	0.127	0.149(5)	0.1386	0.1355	0.1244	--
	Fraction / %	2.6	4.8	18.5(5)	27.8	41.7	16.9	--
LS#2	δ / mm s^{-1}	--	--	--	0.4551	0.4479	0.4620	0.4779(7)
	ΔE_Q / mm s^{-1}	--	--	--			0.0913	0.091(5)
	Linewidth / mm s^{-1}	--	--	--	0.1386	0.1355	0.1244	0.127(2)
	Fraction / %	--	--	--	8.0	6.1	56.6	100

[a] This parameter was fixed during the fit.